

GAIT PHASE IDENTIFICATION OF THE EQUINE GAITS WALK AND TROT USING BOTH WEARABLE AND CAMERA-BASED TECHNOLOGIES

Master Thesis in Electrical Engineering

Rebecka Elander

MASTER THESIS 2022

Gait phase identification of the equine gaits walk and trot using both wearable and camera-based technologies

Rebecka Elander



CHALMERS
UNIVERSITY OF TECHNOLOGY

Department of Physics
Division of Material Physics
CHALMERS UNIVERSITY OF TECHNOLOGY
Gothenburg, Sweden 2022

Gait phase identification of the equine gaits walk and trot using both wearable and camera-based technologies

Rebecka Elander *Master Thesis in Biomedical Engineering*

© Rebecka Elander, 2022.

Supervisors:

KARLSTEEN Magnus, Department of Physics

`magnus.karlsteen@chalmers.se`

SIDDHARTHA Khandelwal, VectorizeMove AB

`hello@vectorizemove.com`

ROEPSTORFF Lars, Swedish University of Agricultural Sciences

`lars.roepstorff@slu.se`

Examiner: Magnus Karlsteen, Department of Physics

Master Thesis 2022

Department of Physics

Division of Material Physics

Chalmers University of Technology

SE-412 96 Gothenburg

Telephone +46 31 772 1000

Cover: Illustrations of a horse walking (top) and trotting (bottom). Author's own illustrations

Typeset in L^AT_EX

Printed by Chalmers Reproservice

Gothenburg, Sweden 2022

Gait phase identification of the equine gaits walk and trot using both wearable and camera-based technologies

Rebecka Elander

Department of Physics

Chalmers University of Technology

Abstract

Healthy gait consists of locomotion, balance and the ability to adapt to the environment. The human gait cycle has been studied thoroughly and gait analysis has been used for various applications. The biomechanics of the horse is well-known, but there is a need to develop systems that can quantify the quality of equine gait, especially in the real world. Inertial Measurement Units (IMU's) are small, lightweight, and ambulant sensors which can determine the position and orientation of the body segments they have been placed on.

The aim of this study was to investigate the possibility of using an Inertial Measurement Unit (IMU) System, especially placed at the cannons, to identify the gait phases for walk and trot, and to use an Optical Motion Capture System to validate these with information from wearable sensors.

The positions of the hooves and cannons were tracked using Qualisys Track Manager. The resultant acceleration of each position was calculated. The resultant acceleration of Movebeat's acceleration data, was computed in each sample. Hoof Strikes and Toe Offs were detected using Tracker from video recordings from Qualisys.

The acceleration patterns were similar for Movebeat and Qualisys for both hooves and cannons and the acceleration peaks almost coincided with Hoof Strike and Toe Off. However, there were some parts of the pattern that differed, where one probable explanation could be that the acceleration from Qualisys was estimated, while the acceleration from Movebeat was measured.

The conclusions are that IMU's placed on the cannons are able to identify the gait events for walk and trot with accuracy, and that Hoof Strike and Toe Off almost coincides with the acceleration peaks. However, further investigations of the accelerations and the gyros in the different directions, x, y and z, need to be done to simplify the identification of the gait phases. More studies need to be performed to further validate the consistency of the identifications.

This study was a collaboration project between Chalmers University of Technology, Swedish University of Agricultural Sciences, and VectorizeMove AB.

Keywords: equine gait analysis, equine, gait, gait phase identification, walk, trot, IMU, biomechanics.

Acknowledgements

Thank you Agnes, Jenniemy, and Jennie for taking the time and effort to bring your lovely horses to the tests!

Thank you Bojan, Cecilia, and Jackson, for your seemingly endless patience during the cold hours of testing!

Thank you Lars for sharing your expertise with me!

Thank you Magnus for your late night replies, for always bringing out the best in me and for always having my back!

Thank you Sid for your dedication, for sharing your deep knowledge, and for always believing in me!

I would also like to thank the awesome team at VectorizeMove for providing me everything I needed, and to Qualisys support team, for giving me amazing support.

Rebecka Elander, Gothenburg, December 2020

Contents

List of Figures	xi
List of Tables	xiii
1 Introduction	1
1.1 Aim of the study	2
2 Theory	3
2.1 Gait Analysis	3
2.2 Equine gaits	5
2.2.1 Walk	6
2.2.2 Trot	6
2.2.3 Canter	7
2.3 Equine Biomechanics	7
2.3.1 Movement of the front leg	8
2.3.2 Movement of the hind leg	10
2.4 Inertial systems	11
2.4.1 MEMS Accelerometers	12
2.4.2 Limitations of Inertial systems	12
2.5 Optical Motion Capture Systems	12
2.5.1 Limitations of Optical Motion Capture Systems	13
3 Methodology	15
3.1 Test Protocol	16
3.1.1 Equipment	16
3.2 Pre-Processing	18
3.3 Analysis	20
3.4 Walk	20
3.5 Trot	27
4 Results	33
4.1 Walk	33
4.2 Trot	35
5 Discussion and Conclusions	37
5.1 Future Work	39

List of Figures

2.1	The different phases in the human gait cycle. Adopted from [1] . . .	4
2.2	An illustration of kinetics, kinematics and spatio-temporal in walk for human (a) and equine (b)	5
2.3	Illustration of a horse performing trot. Author's own illustration . . .	7
2.4	Illustration of a horse performing left lead canter. Author's own illustration	7
2.5	Schematic illustration of the joints of the front leg (a) and the hind leg (b) of a horse. Author's own illustration	8
2.6	A schematic illustration of a setup for an optical motion capture system (a) and a setup in a real environment (b)	13
3.1	Flowchart of the project	15
3.2	The riding hall at Ultuna, SLU, as an illustration (a), and when performing a real test	17
3.3	The equipment of the horse seen as an illustration (a) and in the real test environment (b)	17
3.4	The placement of equipment of the horse - the hooves and the cannons (a), on the croupe and the wither (b), and on the head and the neck (c)	18
3.5	Qualisys' markers inside the red squares to the left, and Movebeat's sensors inside the blue squares to the right	18
3.6	The acceleration by Qualisys for hooves and cannons with the HS (red) and TO (green) manually verified with Tracker	21
3.7	The acceleration measurements from the cannons and the hooves using Movebeats system with the HS (red) and TO (green) manually verified with Tracker	22
3.8	The estimated acceleration by Qualisys and the measured acceleration by Movebeat for the hooves in (a), and the gait diagram for walk in (b), together with HS (red) and TO (green) manually verified with Tracker	23
3.9	One complete step of front left in walk	24
3.10	The acceleration of front left hoof and cannon using Qualisys' calculated acceleration (a) and Movebeat's measured acceleration (b) . . .	25
3.11	One complete step of hind left in walk	26
3.12	The acceleration of hind left hoof and cannon using Qualisys' estimated acceleration (a) and Movebeat's measured acceleration (b) . .	26

3.13	The acceleration calculated from measured positions using Qualisys for hooves and cannons in with the HS (red) and TO (green) manually verified with Tracker	27
3.14	The acceleration measurements from the cannons and the hooves using Movebeat’s system with the HS (red) and TO (green) manually verified with Tracker. The gait diagram is displayed in (c)	28
3.15	The estimated acceleration from Qualisys and measured acceleration from Movebeat, of the hooves together with HS (red) and TO (green) manually verified with Tracker	30
3.16	One complete step of front left in trot	31
3.17	The acceleration of front left hoof and cannon using Qualisys’ calculated acceleration (a) and Movebeat’s measured acceleration (b) in trot	31
3.18	One complete step of hind left in trot	32
3.19	The acceleration of front left hoof and cannon using Qualisys’ calculated acceleration (a) and Movebeat’s measured acceleration (b) in trot	32

List of Tables

2.1	The sagittal plane motion of the front leg joints	9
2.2	The sagittal plane motion of the hind leg joints	10
3.1	The performed tests with duration and how many times each test was repeated	16
3.2	An overview of the specifications of Qualisys and Movebeat	19

Definitions

Beat

Footfall of a hoof or a diagonal pair of hooves that strike the ground virtually simultaneously. The walk has four beats per stride, the trot has two beats per stride, and the canter has three beats per stride

Extension

The movement by which the two ends of any jointed part are drawn away from each other

Flexion

Articulation of a joint or joints so that the angle between the bones becomes smaller

Kinematics

The branch of mechanics that is concerned with the description of movements

Kinetics

Energy of a body related to translational and rotational movement

Rhythm

The recurring characteristic sequence and timing of footfalls and phases of a gait. For purposes of dressage, the only correct rhythms are those of the pure walk, trot, canter, rein back and piaffe

Spatio-temporal

Of or relating to both space and time

1

Introduction

Gait is defined as the pattern of steps in a particular speed [2], and healthy gait consists of locomotion, balance and the ability to adapt to the environment [3]. Gait is one of the main functional activities that is required to accomplish routines of everyday life [4] and maintain well-being [5]. Deviations from normal gait could be an indication of dysfunction in the neuro-physiological systems involved, or improper coordination [6], which makes gait analysis a valuable tool in various applications.

Gait analysis has been a fundamental method to characterize human locomotion [7], and the human gait cycle has been studied thoroughly [7, 8]. Further, gait analysis has been applied to enhance athlete's performance in sports training, to monitor the patient's healing process in rehabilitation, and has been used as an ambulatory method to monitor patients with mobility related disorders.

The biomechanics of the horse is thoroughly studied and well-known [9], and the existing methods of gait analysis are considered highly valuable tools for researchers. However, there is a need to develop systems that can quantify the quality of gait [10, 11], not just in clinical settings, but especially in the real world [6]. Realworld conditions may be quite different and difficult to simulate inside lab facilities, since gait in everyday life may involve varying speed and different surfaces [6]. Systems that can monitor continuously in everyday life environments, could potentially initiate newer interventions and improve existing decision-support systems [6].

Optical Motion Capture systems are considered the gold standard to

quantify kinematics [12]. However, these systems require a significant number of cameras and supporting infrastructure, which increases the cost and limits the applications of the systems to a fixed place where the examinations needs to be performed. An inertial measurement unit (IMU), however, is a low-cost, small, light-weight and ambulant sensor, typically containing a tri-axial accelerometer, a tri-axial gyroscope, and a tri-axial magnetometer [12]. By placing an IMU onto a body segment, the position and orientation of that specific body segment can be determined [6, 12]. This allows kinematic evaluation of motion in realistic environments and conditions, and decreases the operational constraints compared to Optical Motion Capture systems [12]. According to [13], an IMU can be applied to many body regions accurately and reliably, however, the degree of reliability is dependent of the IMU system and which specific anatomical site is being used. To simplify the test environment for the user, there should be an easy way to place the IMU correctly. Ideally, the IMU should be placed on the hooves, but there is no obvious solution of how to put an IMU on the hoof easily. The cannon is, however, a possible option. There are specific shin-guards made for horses which are placed on the cannon, which makes it a possibility to simplify the correct placement of an IMU at the cannons. However, the knowledge of how to analyse the movement with an IMU placed at the cannon, is limited.

1.1 Aim of the study

- Investigate the possibility of using IMU's, especially placed at the cannons, to identify the gait phases in walk and trot
- Validate the accuracy and consistency of the identified gait phases with information from wearable sensors using an Optical Motion Capture System

This project is a collaboration between Chalmers University of Technology, Swedish University of Agricultural Sciences, and Vectorize-Move AB.

2

Theory

In this section, the field of gait analysis is further explained, along with the Equine gaits and biomechanics.

2.1 Gait Analysis

Gait analysis includes the measurement, description, and assessment of quantities that characterize the locomotion [7]. Normal gait consists of three primary components: locomotion, balance and ability to adapt to the environment and requires a balance between various interacting neural systems [14]. One step in human gait includes the right initial contact, or heel-strike, left pre-swing, left initial contact, or heel-strike, and right pre-swing [6, 1], viewed in figure 2.1. When focusing on just one leg, the step of a horse follows the same pattern [9]. However, a horse has four legs, which makes the equine gait more challenging when compared to the human gait [9]. The two main gait phases are the stance phase and the swing phase. The stance phase refers to the part of the step where the leg is in contact with the ground, whereas the swing phase refers to the part of the step where the leg is free from contact with the ground [9]. The stance phase starts with the initial ground contact (heel-strike for humans), followed by the loading response, the mid-stance, and ends with the pre-swing [9]. After the pre-swing, the swing phase begins with the initial swing, followed by the mid-swing, and ends with the terminal swing [9].

In walk, there is always at least one hoof on the ground [9], as can be viewed in the illustration in figure 2.2. However, when studying trot, figure 2.3, or canter, figure 2.4, one (canter) or two (trot) moments

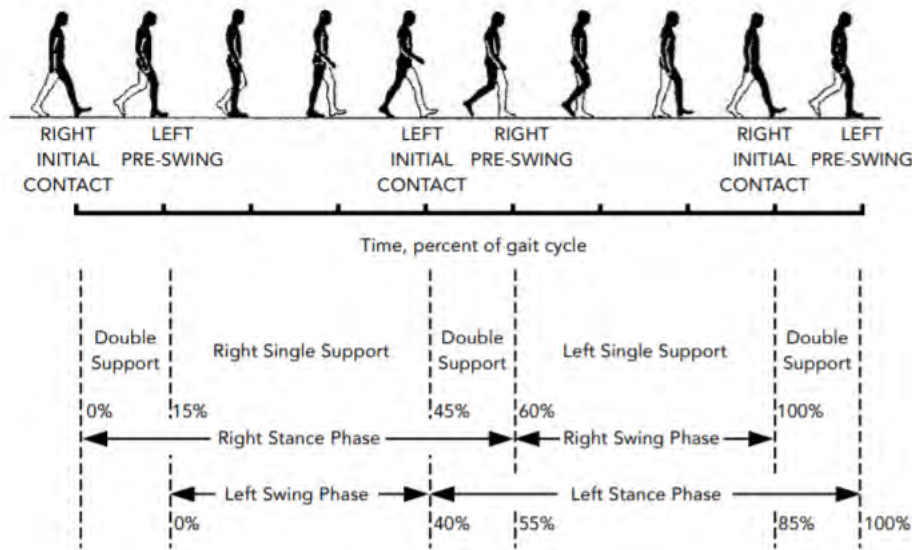
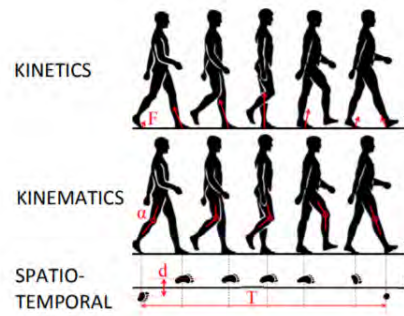


Figure 2.1: The different phases in the human gait cycle. Adopted from [1]

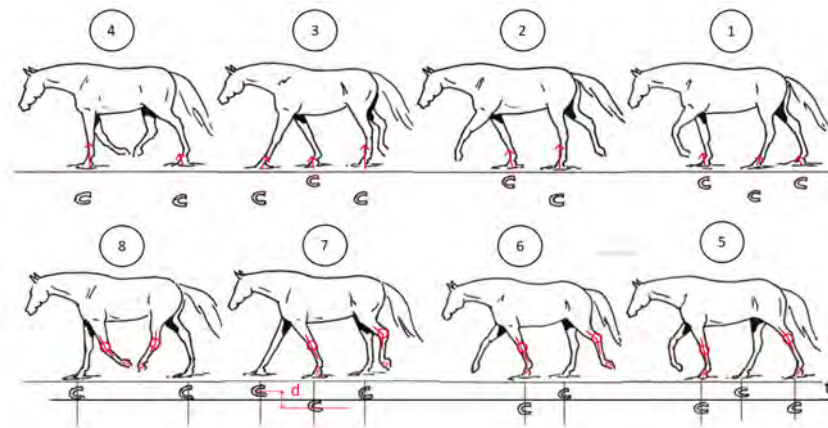
of suspension are present in one step of the horse [9]. A moment of suspension is defined by all four legs being in the swing phase simultaneously and hence free from weight bearing [9].

Kinematic data include variables that are temporal, linear and angular [9], and the displacement and orientation of body segments, joint angles and spatio-temporal gait parameters [15]. Spatio-temporal parameters include both spatial parameters, relating to the position such as step length, and temporal parameters, relating to time, such as stride time [6]. According to [9], the frame numbers and sampling frequencies can be used to calculate temporal data such as the stride duration and the limb coordination patterns. When combining the calibration information with the coordinates of the markers, distance data which describes the stride length, the distances between limb placement, and the flight of the body parts, can be computed. The displacements, velocities and accelerations of the body segments and joints are described by angular data.

The kinetic analysis include the external and internal locomotor forces, lower limb joint mechanical moments and powers, kinetic and potential energy [15], by using accelerometers and gyroscopes to record the movements of the limb segments [16, 9]. These movements are rotations produced in the limb segments by muscle generated forces [9].



(a) Explanation of kinetics, kinematics and spatio-temporal. Adopted from [17] with permission



(b) Explanation of kinetics, 1-4, kinematics, 5-8, and spatio-temporal, the steps of the hooves below 5-8, of a horse. Author's own illustration

Figure 2.2: An illustration of kinetics, kinematics and spatio-temporal in walk for human (a) and equine (b)

Figure 2.2 illustrates an explanation of the kinetics, kinematics, and spatio-temporal aspects of human (a) and equine (b) gait.

2.2 Equine gaits

According to [18], gaits are classified as symmetrical or asymmetrical. Further, quadrupedal mammals often use symmetrical gaits for slow running, and asymmetrical gaits for fast running, where trot is the most common symmetric running gait. However, there are exceptions, such as camels which pace, and elephants which amble instead of trot. Walking is only performed at low speed.

The gaits of the horse include the symmetric gaits, such as walk, trot, running walk, rack, toelt, fox trot, paso, and stepping pace, and the asymmetric gaits, such as canter, transverse and rotary gallop, and half bound [9]. A symmetric gait is defined by that the footfalls of the left and the right side and the fore and hind limbs are evenly spaced in time, while in an asymmetric gait, the footfalls of the fore and/or hind limbs is coupled to each other [9]. In this report, walk, trot, and canter will be investigated further, since these gaits are the main gaits used in Swedish Warmblood riding horses.

2.2.1 Walk

The walk has a four-beat rhythm [9, 18], and is a symmetric gait [9] given by its footfall sequence - hind right, fore right, hind left, fore left [19]. The sequence of the walk is illustrated in figure 2.2(a) (human), and 2.2(b) (equine). Walk is the slowest gait, and the stride consists of large overlap times between the legs' stance phases, without any suspension period [9]. The variability of these overlaps is probably one of the reasons that the walk is considered to be the most complex equine gait [9]. When observing six highly trained dressage horses, only one of these had a regular four beat rhythm of the footfalls [20].

There are four different types of walk in dressage competitions; collected walk, medium walk, extended walk and free walk [20].

2.2.2 Trot

Trot is a two-beat symmetric gait [9, 18, 19] where diagonally opposite legs swing, almost, at the same time [19]. The footfall sequence is; right hind together with left fore followed by left hind together with right fore [19], as illustrated in figure 2.3. There is a slight difference in the diagonal placement in collected trot in elite dressage horses, where the hind limb hits the ground approximately 20-30 ms before the diagonal fore limb [21, 22]. There are four different types of trot; collected trot, working trot, medium trot, and extended trot, where the speed increases from collected to extended trot [9, 20].

Piaffe and passage are derived from collected trot, and are also diagonal exercises [23]. According to [23], the stride duration is longer

for piaffe and passage than for collected trot, which implies that the stride frequency is lower. Further, the passage had a lower speed and stride length and in passage, the diagonal advancement increased by approximately 9.7 ms. Collected trot and passage are very similar to each other regarding other temporal variables, but the suspension phase was found to be shorter in passage [23].

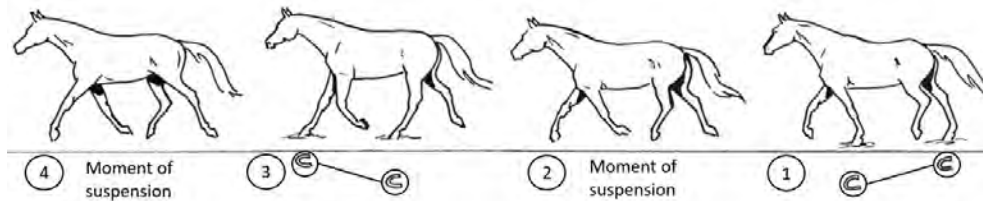


Figure 2.3: Illustration of a horse performing trot. Author's own illustration

2.2.3 Canter

Canter is an asymmetric gait with a three-beat rhythm [9]. There are four variations of canter in dressage; collected canter, working canter, medium canter and extended canter, where the speed of the gait increases from collected to extended canter. There are two possible footfall sequences in canter, one for the right lead canter, and one for the left lead canter [9]. For right lead canter, the footfall sequence is; left hind limb, right hind limb together with left fore limb, and lastly right fore limb. In left lead canter, the footfall sequence is; right hind limb, left hind limb together with right fore limb, and lastly left fore limb. The footfall sequence of canter is illustrated in figure 2.4

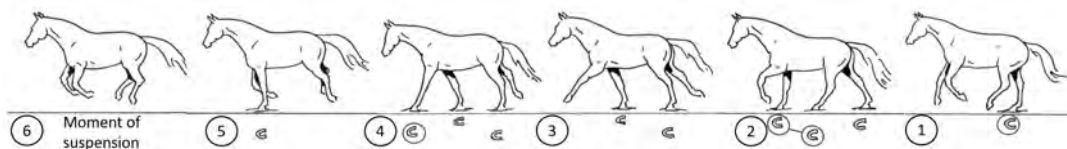


Figure 2.4: Illustration of a horse performing left lead canter. Author's own illustration

2.3 Equine Biomechanics

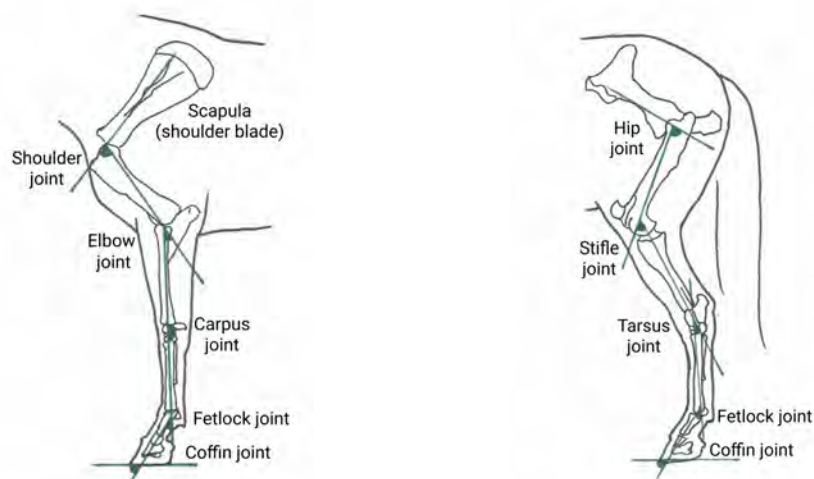
According to [24], the definition of biomechanics are "the physical forces that affect human and animal movement, or the study of these

forces". To benefit from the locomotor apparatus of the horse, the humans domesticated horses [9]. Further, the selective breeding, made it possible to produce different types of horses - heavier draught horses were selected to help the humans to pull heavy carts, and more slender and faster horses were selected for their speed and endurance. The importance of the locomotor apparatus of the horse is once again highlighted, since the sport horses of today are described as "equine athletes" [9].

Flexion and extension are rotations made in the sagittal plane, where the flexion is referring to the movement that decreases the angle between two body parts, and extension is referring to the movement where the angle between two body parts increases [25].

2.3.1 Movement of the front leg

From the elbow and distal, the horse's front leg is more or less constrained to move in the sagittal plane [9]. Table 2.1 presents the movement of the different joints of the front leg in one stride in trot. The joints included in the front leg movement are the scapula, the shoulder, the elbow, the carpal joint (carpus), the fetlock joint, and the coffin joint [9], as seen in figure 2.5a.



(a) An illustration of the joints of the front leg

(b) An illustration of the joints of the hind leg

Figure 2.5: Schematic illustration of the joints of the front leg (a) and the hind leg (b) of a horse. Author's own illustration

Table 2.1: The sagittal plane motion of the front leg joints

Stride - front leg sequence in trot								
	Stance					Swing		
	Initial Contact	Loading Response	Mid Stance	Terminal Stance	Pre-Swing	Initial Swing	Mid Swing	Terminal Swing
Scapula	Max flexion	Gradually extracts			Maximal	extraction	Gradually flexes	
Shoulder	Almost fully extended	Max flexion	Extends			Extends	Extends	Flexes
	Elastic energy storage and release			Active propulsion				
Elbow	Extended	Flexes	Flexes	Extends	Max extension	Max flexion		Extends
	Power absorption peak						Power generation peak	
Carpus Coffin	Slightly flexed	Extends	Max extension	Flexes	Rapid flexion		Max flexion	Extends
	Extends	Extends	Max extension			Flexes	Extends	Flexes
	Energy absorption			Energy release				
Fetlock		Max flexion			Max extension	Flexion peak		
	Peak power absorption			Power release				

During the stride, the rotation of the scapula is extracting and protracting with a sinusoidal pattern. At the initial ground contact, the scapula reaches its maximal protraction, and at the end of the stance phase, the maximal extraction occurs.

Unlike the scapula, the shoulder is almost fully extended at the initial ground contact, but during the loading response, the joint rapidly flexes to its maximum. After the maximum flexion at the loading response, the shoulder extends more or less during the rest of the stance phase and the most of the swing phase, until the front leg reaches the terminal swing phase, where the shoulder joint begins to extend again.

At the initial ground contact, the elbow is extended. Through the loading response it flexes, but near the end of the stance phase it extends to its maximum. The maximal flexion occurs in the early swing phase, and during the swing phase it undergoes a flexion cycle. In the initial ground contact, the power absorption peaks and in the mid swing, the power generation peaks.

When the carpal joint hits the ground at the initial ground contact, it is still flexed, but it rapidly extends in the early stance. At the mid stance, there is a second extension peak, right after a plateau. After the second extension, the carpal joint starts to flex rapidly before the end of the stance phase. Throughout the swing phase, there is a flexion cycle, until the later part, where the joint extends again, preparing for the initial ground contact.

Table 2.2: The sagittal plane motion of the hind leg joints

Stride - hind leg sequence in trot								
Stance					Swing			
	Initial Contact	Loading Response	Mid Stance	Terminal Stance	Pre-Swing	Initial Swing	Mid Swing	Terminal Swing
Hip		Gradually extends			Max extension	Gradually flexes		Max flexion
		Energy generation			Energy absorption			
Stifle	Extended, rapidly flexes	Energy generation					Max flexion	Extends
Tarsus	Extended, rapidly flexes				Energy absorption		Flexion peak	Extends
	Energy absorption							
Fetlock	Extends	Rapidly extended	Max extension			Max flexion peak	Slight extension, followed by a flexion peak	Extends
	Energy absorption					Energy generation		
Coffin	Flexes	Flexion peak				Max extension	Flexion peak	Extends

The fetlock joint rapidly extends after the initial ground contact, and then plateaus. During the early stance, the joint extends again, and eventually reaches its maximal value at mid stance. The swing phase contains two peaks of flexion, with a slight extension that separates the two. At the end of the swing phase, the extension stops rapidly.

When the hoof hits the ground, the coffin joint starts to flex. Just before the mid stance, the flexion of the joint is at its max. In the late stance, the coffin joint is maximally extended, and shifts rapidly to a flexion peak at the early swing phase.

2.3.2 Movement of the hind leg

Table 2.1 presents the movement of the different joints of the front leg in one stride in trot. The joints that are included in the hind leg's movement are the hip joint, the stifle joint, the tarsus joint, the fetlock joint and the coffin joint [9], as seen in figure 2.5b. The movement of the hip joint has a sinusoidal pattern throughout the stride. Before the end of the stance phase, the hip joint extends maximally, and near the end of the swing phase, the maximal flexion occurs.

The stifle joint flexes rapidly during the loading phase. Maximal flexion appears near the mid swing.

At the beginning of the stance phase, the tarsal joint is rapidly flexed, and reaches a peak of flexion. The maximal extension happens somewhere in the late stance phase. Near the mid swing, there is a peak

in flexion, just after passing the angle at square stance in the early swing.

The fetlock joint extends rapidly at the initial ground contact, and reaches its maximal extension at mid stance. In the early swing phase, the maximal flexion appears. After this maximum, there is a slight extension in the mid swing, and a second flexion peak followed just after. The joint extends at the end of the swing phase to prepare for the initial ground contact.

The rapid loading of the limb at the beginning of the stance phase forces the coffin joint to flex. Just before mid stance, the flexion peaks. When the heel lifts, at the initial swing phase, the extension reaches its maximum. Further, the joint rapidly flexes to a small flexion peak, and then reaches a peak flexion at the mid swing. Before hitting the ground at the initial ground contact, the joint extends.

The tendons of the hind leg are used as springs to conserve the energy during the stride [26]. The synchronized flexion peaks in the stifle and tarsal joints absorbs the shock from the vertical ground force [26]. The flexion peaks of both the fetlock joint and the coffin joint also contributes to the shock absorption [27].

2.4 Inertial systems

Inertial systems use the acceleration and orientation in three axis and integrate over time to track the position and orientation of an object relative to a known starting point, orientation, and velocity [16]. The inertial measurement units (IMU) provides the measurements of angular velocity and linear acceleration by using three orthogonal gyroscopes and accelerometers [16].

The inertial sensors used in this report are microelectromechanical systems (MEMS) sensors. Therefore, the sensors presented in this section will be MEMS.

2.4.1 MEMS Accelerometers

There are a lot of advantages using MEMS accelerometers, including the small size and light weight, the low start-up time and the low power consumption [16], hence they are used in this report. The MEMS accelerometers use the same principals as the mechanical and the solid-state devices [16]. The mechanical accelerometers use Newton's second law $F=ma$ to calculate the acceleration acting on the device. The traditional mechanical accelerometers are made of mass suspended by strings, and the displacement pick-off is measured by the displacement mass, which gives the signal proportional to the force F .

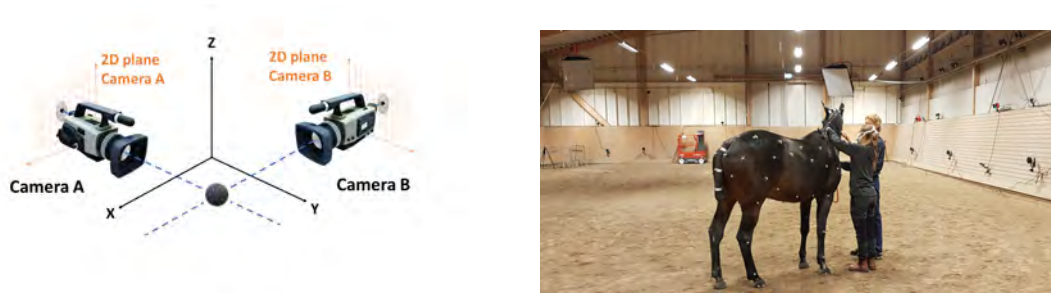
2.4.2 Limitations of Inertial systems

The main disadvantage when using MEMS accelerometers, is that they are not as accurate as the traditional mechanical and solid-state accelerometers [16]. According to [16], there are five main sources of errors in MEMS sensors; constant bias, white noise, temperature effects, calibration, and bias instability. The errors from using the accelerometers need to be integrated twice to track the position, which differs from the gyroscopes, which only need to be integrated once [16].

2.5 Optical Motion Capture Systems

When tracking an object with Optical Motion Capture Systems, multiple cameras are used to detect infra-red light being either reflected or emitted from markers placed on the object [28]. Further, there is a need to record the position of the markers at a high frame rate, to be able to track the movements of the object in detail. Passive markers are typical spherical balls with retro-reflective coatings that are placed on the object and reflect infra-red light that are emitted parallel to the axis of the camera from light sources around the camera's lens [28]. Active markers, on the other hand, emit light actively which the camera detects. This means that active markers need to be wired to be able to emit the light [28].

One camera can only identify the motion of a marker in a 2D plane, as illustrated in figure 2.6(a), and cannot provide information of the motion in the plane that is perpendicular to the axis [28]. Because



(a) A schematic illustration of a setup for an optical motion capture system. Author's own illustration with inspiration from [28]

(b) A setup of an optical motion capture system in a real environment. Accessed from author's own collection

Figure 2.6: A schematic illustration of a setup for an optical motion capture system (a) and a setup in a real environment (b)

of this, the marker needs to be imaged by at least two cameras at all times to be able to identify the position, and hence the motion, of the marker. If two cameras provide information from two nonparallel images, these images can be reconstructed by using stereo triangulation [29]. A setup of a real optical motion capture system is displayed in figure 2.6(b).

2.5.1 Limitations of Optical Motion Capture Systems

The marker needs to be visible to at least two cameras at the time for the system to be able to track the motion of the object in 3D. The cameras lose track of the marker or confuse it with another marker if it is occluded by body segments. The problem can be reduced by adding more cameras, however, the more cameras the more complex system, and the problem will not be completely solved anyway. Even if knowledge of human body constraints, signal processing techniques, and optimization methods have helped solving the problem when identifying plausible markers and track momentarily occluded markers, the required setup and algorithms are often too complex, and manual editing is often still necessary when using the system in clinical applications [28]. Other limitations of optical motion capture systems are the high cost of the system, along with the extensive calibration and configuration that is required for each patient when applying it in a clinic [28].

The system needs high quality cameras with high resolution. As the distance between the marker and the camera increases, the smaller the image becomes, which increases the difficulty of capturing the motion of the marker robustly and accurately [28]. Further, the size of the marker, the distance from the camera and the camera's resolution are limitations of the accuracy of the measurement.

Optical systems output the linear and angular position of body segments, which have made it possible to integrate these systems in for example animations, movies and games [28]. Further, these systems have also been used in the biomedical field, such as gait analysis, but since these applications require calculations of kinetic variables, including joint forces and energetics, which are mandatory to obtain the acceleration and velocities from the differentiated position of the object, the noise, especially the high frequency noise, present in the data will be magnified. However, human motion is relatively small, which makes it simple to filter out the high frequency noise with a low pass filter [30].

3

Methodology

In figure 3.1 the flowchart of this project is illustrated. The following sections will describe the steps from designing the test protocol, section 3.1, the pre-processing of the data, section 3.2, to analysis of the data 3.3.

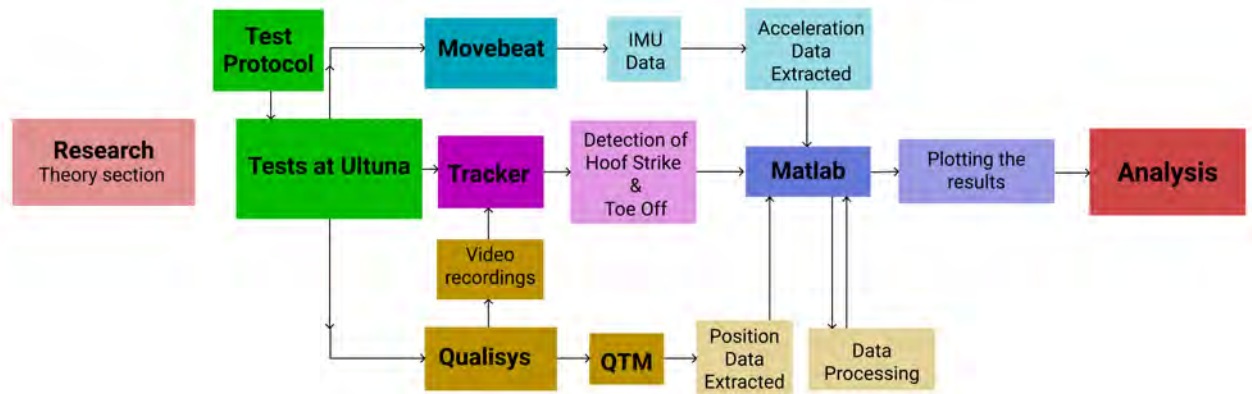


Figure 3.1: Flowchart of the project

The first step was to gain knowledge of what had been done in the field before, and of IMU's and Optical Motion Capture systems, which lead to a minor literature study compiled in the Theory section. Then, a test protocol was designed, see section 3.1, and performed at Ultuna, SLU. Position data was extracted from Qualisys using Qualisys Track Manager (QTM), and only the acceleration data was extracted from the IMU data from Movebeat. The data was then processed for the hooves and cannons. The resultant acceleration of Qualisys' position data was calculated and filtered, and the resultant acceleration of Movebeat's measured acceleration was calculated. Hoof Strikes and

Toe Offs were manually verified from a video recording by Qualisys, using Tracker. The accelerations, Hoof Strikes and Toe Offs were plotted in the same figures.

3.1 Test Protocol

The horse was lounged in a circle in the middle of the arena, with a diameter of approximately 20 m. The tests, with duration and how many times each test was repeated, is presented in table 3.1.

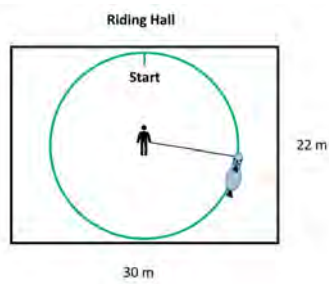
Table 3.1: The performed tests with duration and how many times each test was repeated

Test	Gait	Direction	Duration	Repetitions
a	Walk	Left Hand	90 s	3
b	Walk	Right Hand	90 s	3
c	Trot	Left Hand	90 s	3
d	Trot	Right Hand	90 s	3
e	Canter	Left Hand	90 s	2
f	Canter	Right Hand	90 s	2

The riding hall where the tests were performed had the dimensions of 22m x 30m, as illustrated in figure 3.2. At the beginning of each test, the horse was placed in the middle of the circle, and when the systems were up and running, the systems were time synchronized by knocking three times on the sensor placed at the wither.

3.1.1 Equipment

The equipment setup is illustrated in figure 3.3(a), and displayed at the real test environment in figure 3.3(b). Eleven clusters of markers of Qualisys were used. One cluster of four markers were placed at the neck, figure 3.4(c), and one cluster of three markers was placed at the wither and lumbar each, 3.4(b). At each of the cannons, one cluster of three markers were placed, and one cluster of three markers was placed at the hoof, where one of these markers was placed at the lateral side of each of the hooves, as displayed in figure 3.4(a), and in figure 3.5 to the left.

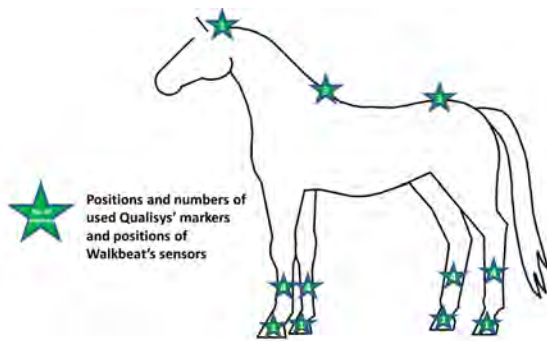


(a) Illustration of the riding hall with the circle in the middle of the arena, with a diameter of approximately 20 m



(b) Test d, trotting in right hand, performed in Ultuna's riding hall

Figure 3.2: The riding hall at Ultuna, SLU, as an illustration (a), and when performing a real test



(a) An illustration of the equipment of the horse in the tests



(b) The equipment of the horse in the real test environment

Figure 3.3: The equipment of the horse seen as an illustration (a) and in the real test environment (b)

In the upper body placement of Movebeat's sensors, these were placed underneath Qualisys' marker in the middle of the clusters - one at the top of the neck, figure 3.4(c), one at the top of the wither, and one at the croupe, figure 3.4(b). Figure 3.4 displays a more detailed overview of the placement of the markers, and figure 3.5 displays a detailed view on the left front leg. The sensors placed on the hooves, was placed on the lateral side of the hoof, with Qualisys' marker on top. The sensors placed on the cannons were placed in the middle of the cannon, anterior to the Qualisys' markers placed in the middle of the cannon. Figure 3.5 presents a more detailed view of the front leg for Qualisys' markers, inside the red squares, to the left, and Movebeat's

sensors, inside the blue squares, to the right.



(a) The setup of the equipment placed on the horse's legs



(b) The setup of the equipment placed on the horse viewed from behind



(c) The setup of the equipment placed on the horse's head

Figure 3.4: The placement of equipment of the horse - the hooves and the canons (a), on the croupe and the wither (b), and on the head and the neck (c)

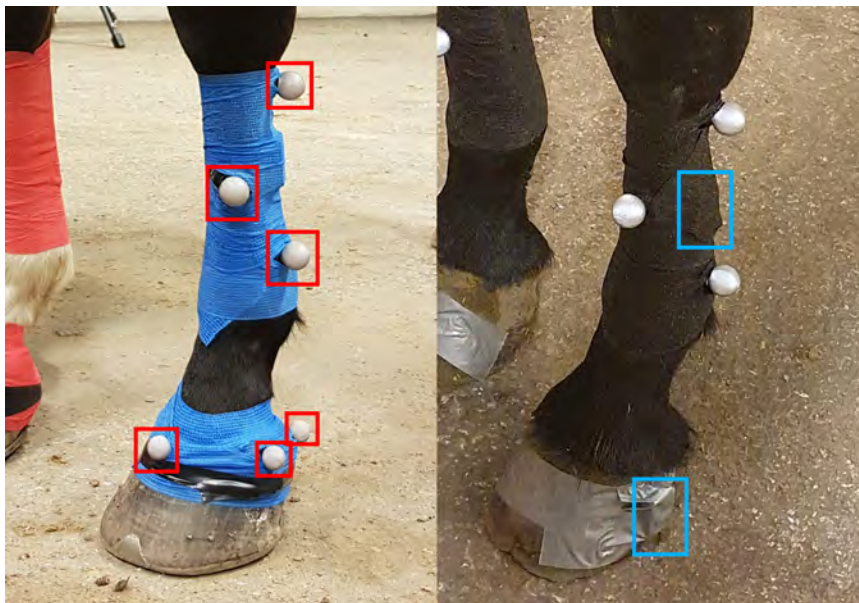


Figure 3.5: Qualisys' markers inside the red squares to the left, and Movebeat's sensors inside the blue squares to the right

3.2 Pre-Processing

Qualisys Track Manager (QTM) was used to track the hooves and the canons of the recording from Qualisys' system. Qualisys Track Manager displays the percentage of samples that were tracked for each

marker, which will further be described as "tracking score". The test with the highest tracking scores for the marker placed on top of Movebeat's sensor on the hooves were selected, one for walk and one for trot, and was further investigated. The same horse was used in the walk test and the trot test, and these were both performed in right hand. The x-, y-, and z-positions of these hoof markers and the marker placed anterior (towards the front of the horse) to Movebeat's sensor on the cannons, were extracted and the resultant acceleration of each of the positions were calculated, filtered by applying median filtering, and plotted using MATLAB, one plot for walk and one plot for trot.

The acceleration data in x-, y-, and z-direction was collected from Movebeat's sensors and visualized using MATLAB. The resultant acceleration of the hooves and the cannons was calculated and plotted, one plot for walk and one plot for trot. The acceleration of the hooves was plotted for both Movebeat and Qualisys in the same figure, one for walk and one for trot.

The Hoof Strikes and Toe Offs were detected manually from Qualisys' video recordings using Tracker, and the sample number for each Hoof Strike and Toe Off were noted and added to the plots.

An overview of Qualisys' and Movebeat's systems is presented in table 3.2.

Table 3.2: An overview of the specifications of Qualisys and Movebeat

System		Sampling frequency [Hz]	No. of Cameras	No. of markers/sensors			Specifications		
				Upper body	Cannons	Hooves			
Qualisys	Optical Motion Capture	Position Tracker	100	32	11	12	12	Relative accuracy Standard deviation of the wand length	0.79269 mm
		Video Recording	30	2					
Movebeat	Inertial Measurement Unit (IMU)		100	-	3	4	4	Acceleration Range Accuracy	± 16 g

3.3 Analysis

Qualisys tracking scores for the hooves in the test in walk were 100.0% for hind left, hind right, and front left, and 99.9% for front right. The tracking scores for the hooves for the selected trot test were 100.0% for hind left and front left, 99.8% for hind right, and 99.3% for front right. All tracking scores for the cannons were 100.0% in both tests.

In the performed tests, Qualisys and Movebeat had a sample rate of 100 Hz for the measured data, and for the videos recorded by Qualisys and analysed using Tracker, the frame rate was 30 Hz. Therefore, the sample number of HS and TO could not be given exact sample numbers, but were instead given an sample interval, as can be viewed in figures 3.6 - 3.8, figure 3.10, figure 3.12, figures 3.13 - 3.15, figure 3.17, and figure 3.19 as thickened lines. In these figures, the stance phase of each leg is marked with a background color, similar to the gait diagram, figure 3.8(b) for walk and figure 3.15(b) for trot.

The acceleration data given by Movebeat has a constant offset of approximately 9.82 m/s^2 when compared to Qualisys' data. This is due to the constant of gravity, g , which is included in the acceleration measurements of Movebeat, but not in the calculated acceleration from measured positions of Qualisys.

The verified Hoof Strike (HS) and Toe Off (TO) from video recordings by Qualisys are consequently colored with red for HS and green for TO.

3.4 Walk

Figure 3.6 presents the acceleration calculated from the positions of the hooves and cannons given by Qualisys and figure 3.7 presents the acceleration of the hooves and cannons given by Movebeat. Both Qualisys' estimated acceleration and Movebeat's measured acceleration of the hooves, are presented in figure 3.8. Hind left (HL) is at the bottom, followed by front left (FL), hind right (HR), and front right (FR). The figures also include TO (red line) and HS (green line) manually verified with Tracker.

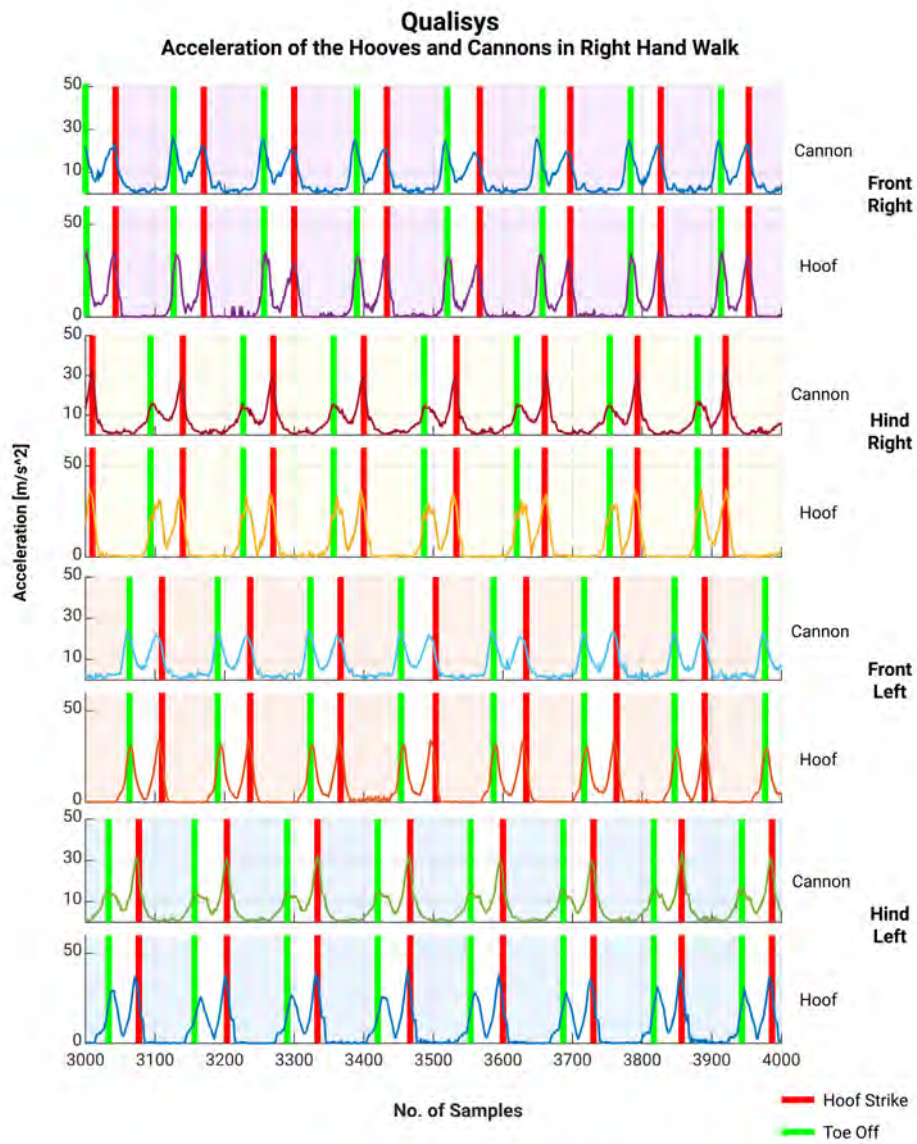


Figure 3.6: The acceleration by Qualisys for hooves and cannons with the HS (red) and TO (green) manually verified with Tracker

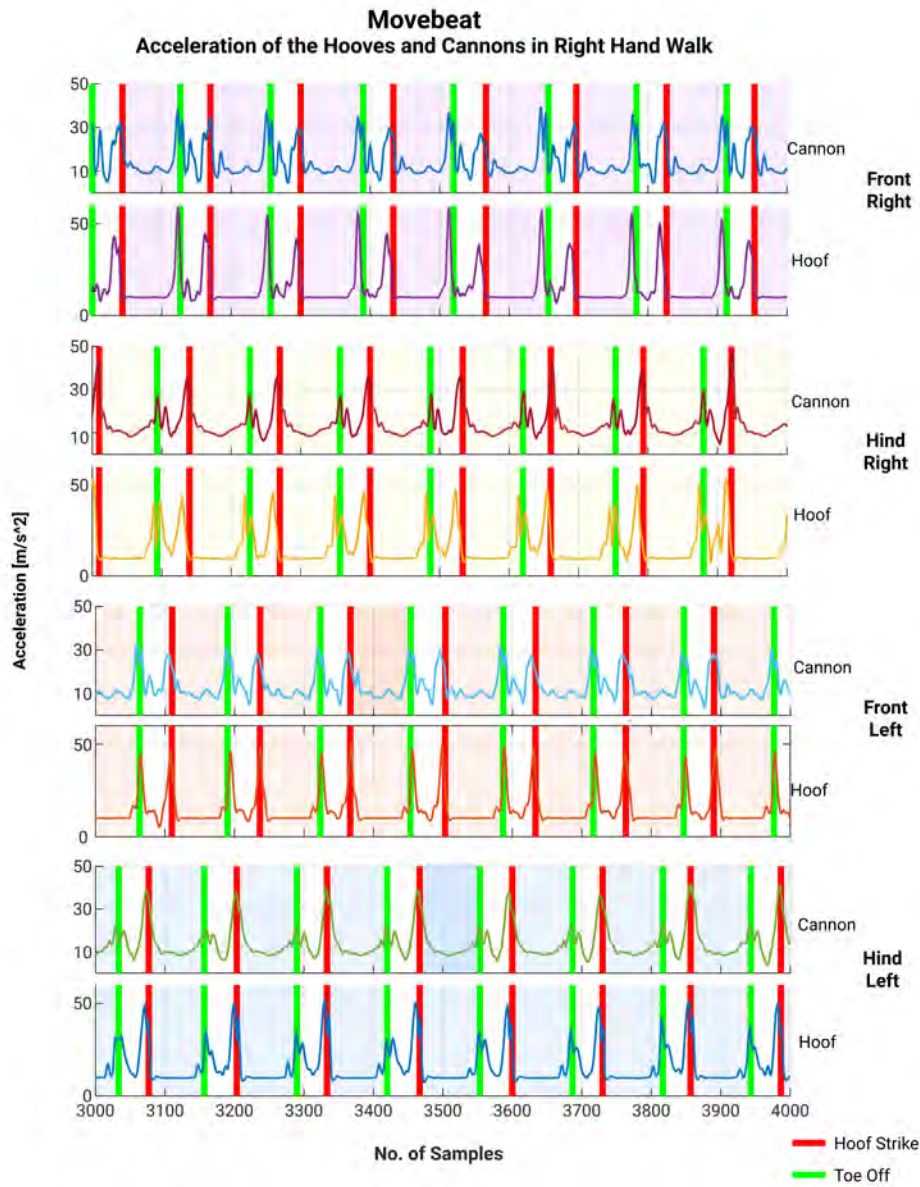
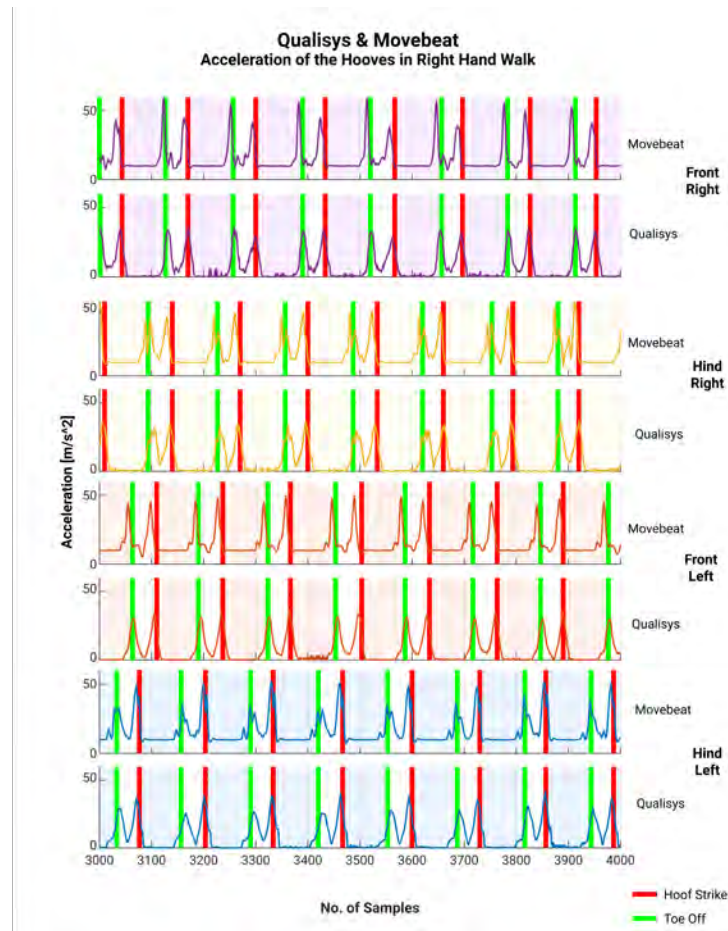
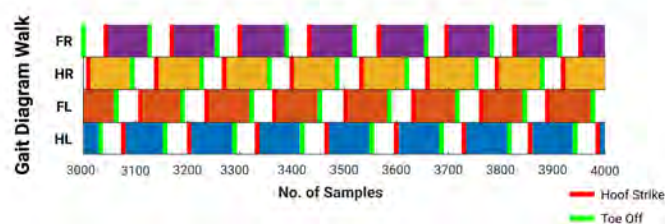


Figure 3.7: The acceleration measurements from the cannons and the hooves using Movebeats system with the HS (red) and TO (green) manually verified with Tracker



(a) The estimated acceleration by Qualisys and the measured acceleration by Movebeat for the hooves together with HS (red) and TO (green) manually verified with Tracker



(b) The gait diagram for walk

Figure 3.8: The estimated acceleration by Qualisys and the measured acceleration by Movebeat for the hooves in (a), and the gait diagram for walk in (b), together with HS (red) and TO (green) manually verified with Tracker

One complete stride of front left is visualized in figure 3.9, starting at the Midstance and going to Pre-Swing in (a), Toe-Off to Terminal Swing in (b), and Initial Contact to Midstance in (c). The print-screens are from a video recorded by Qualisys. In figure 3.10, the same stride as figure 3.9 is displayed, using Qualisys' calculated acceleration (a) and Movebeat's measured acceleration (b).



(a) Midstance to Pre-Swing

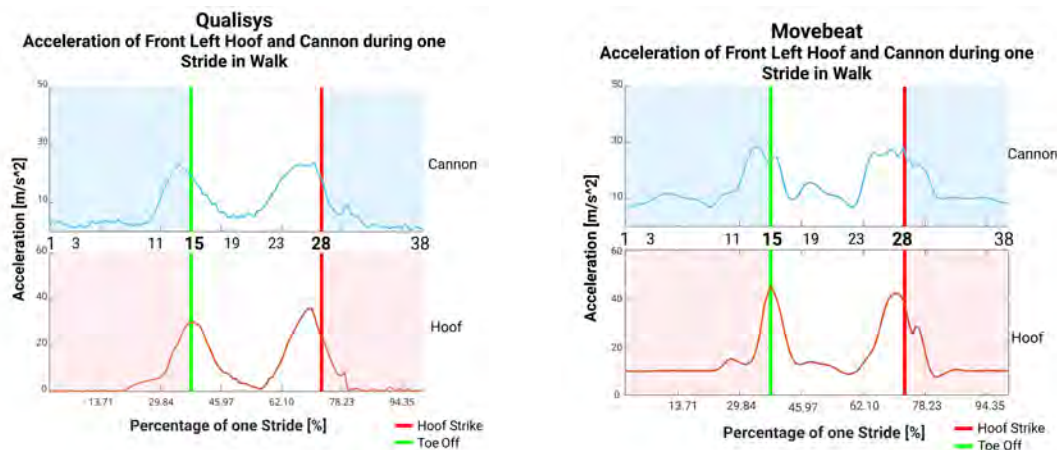


(b) Toe Off to Terminal Swing



(c) Initial Contact to Midstance

Figure 3.9: One complete step of front left in walk



(a) The acceleration of one complete step of front left by Qualisys

(b) The acceleration of one complete step of front left by Movebeat system

Figure 3.10: The acceleration of front left hoof and cannon using Qualisys' calculated acceleration (a) and Movebeat's measured acceleration (b)

Figure 3.11 displays one complete stride for hind left, starting at the Midstance (1), and going to Pre-Swing (14) in (a), Toe-Off (15) to Terminal Swing (27) in (b), and Initial Contact (28) to Midstance (38) in (c). The print-screens are taken from a video from one of Qualisys' cameras. In figure 3.12, the same stride is visualized using Qualisys' estimated acceleration (a) and Movebeat's measured acceleration (b).

3. Methodology



(a) Midstance to Pre-Swing

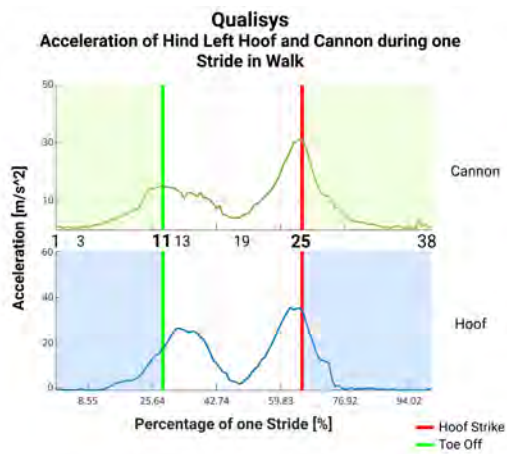


(b) Toe Off to Terminal Swing

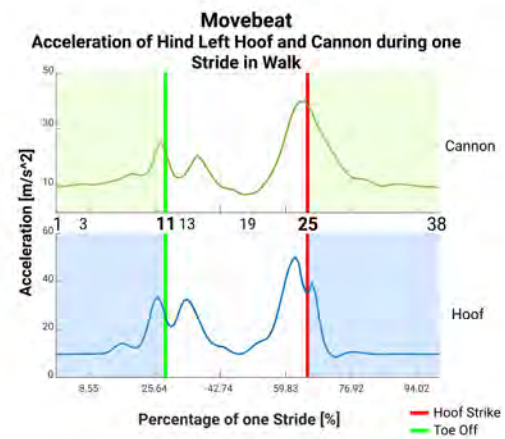


(c) Initial Contact to Midstance

Figure 3.11: One complete step of hind left in walk



(a) One complete step of hind left using Qualisys' system



(b) One complete step of hind left using Movebeat's system

Figure 3.12: The acceleration of hind left hoof and cannon using Qualisys' estimated acceleration (a) and Movebeat's measured acceleration (b)

3.5 Trot

Figure 3.13 presents the acceleration of the hooves and cannons using Qualisys system, and when TO and HS occurs. There are almost five complete strides visualized in these figures. The acceleration data of

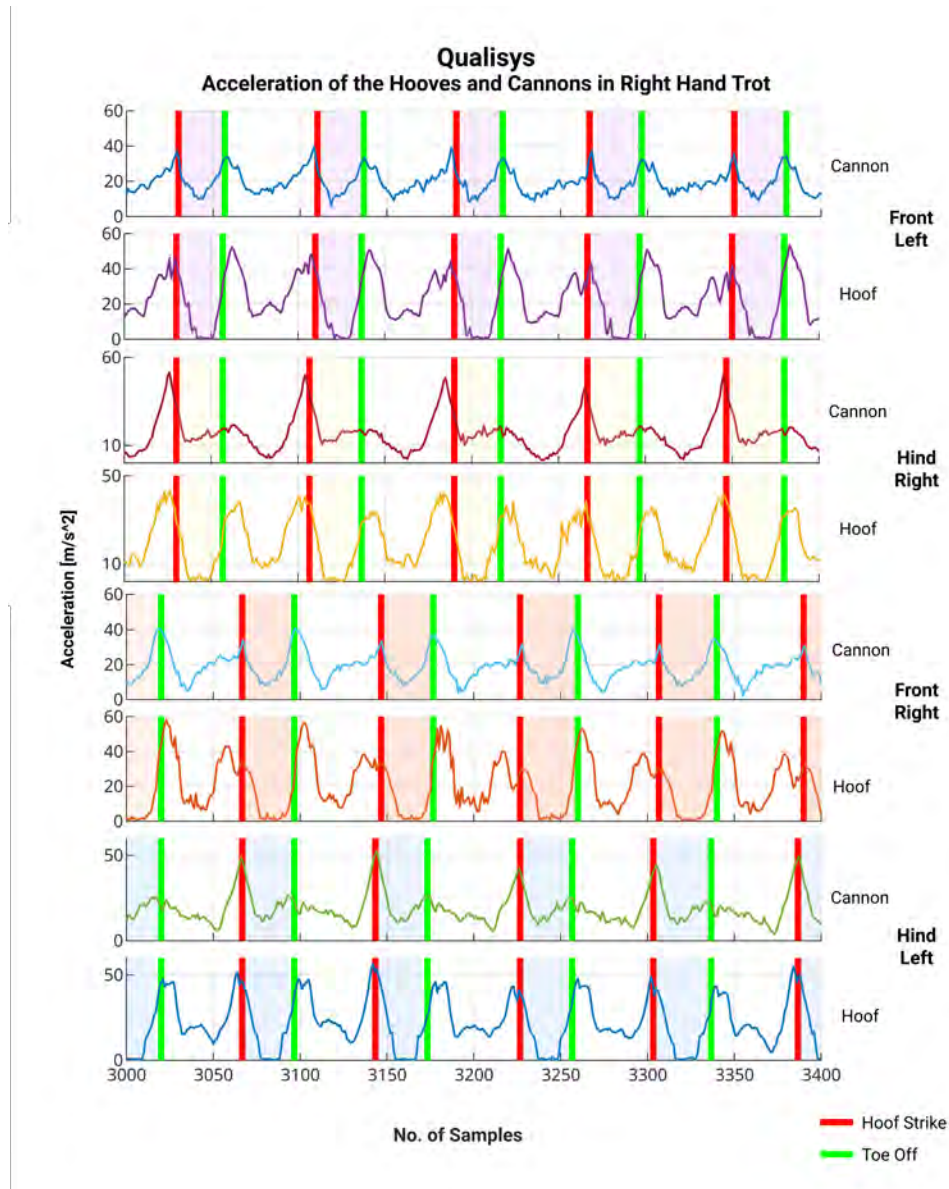


Figure 3.13: The acceleration calculated from measured positions using Qualisys for hooves and cannons in with the HS (red) and TO (green) manually verified with Tracker

the hooves and the cannons in trot collected with Movebeat is presented in figure 3.14.

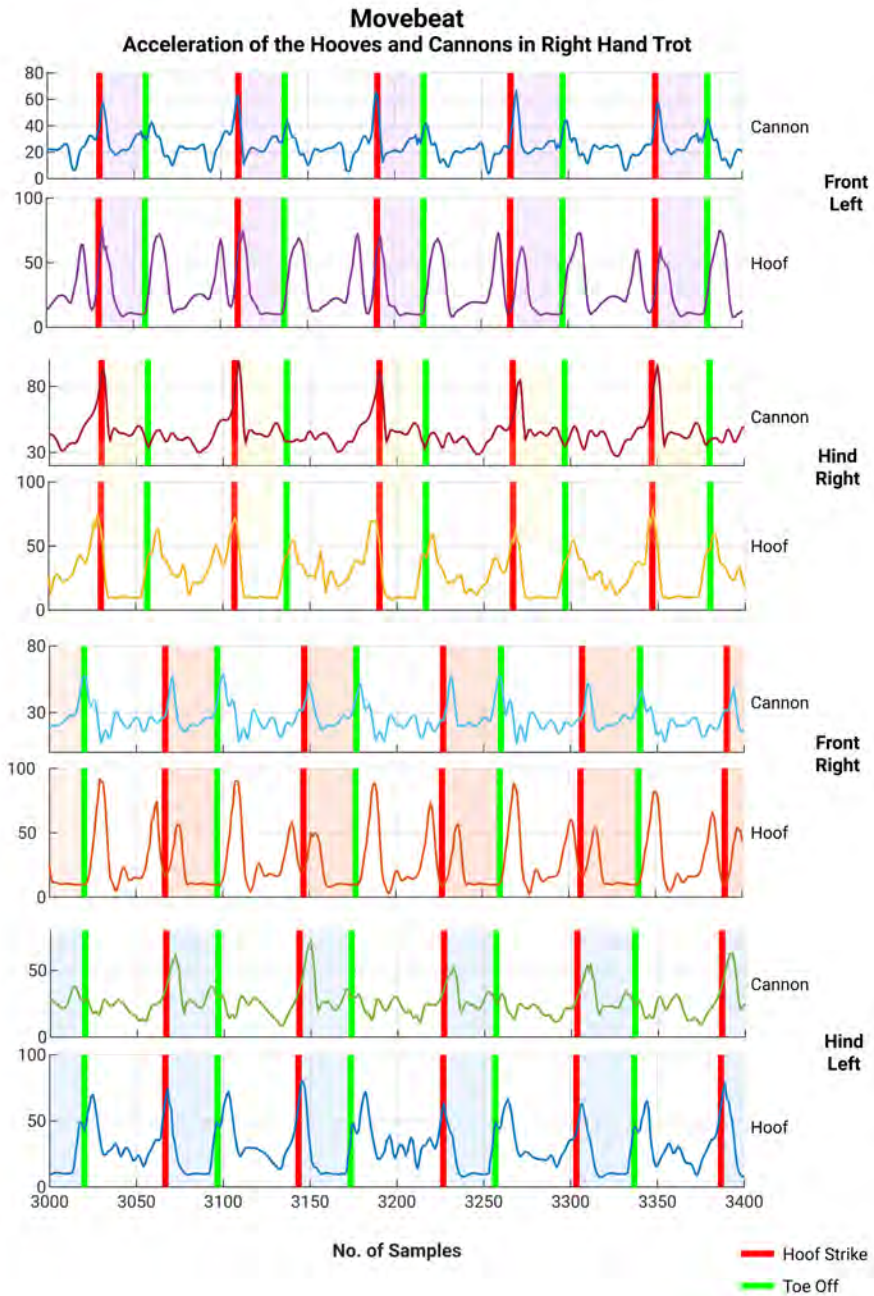
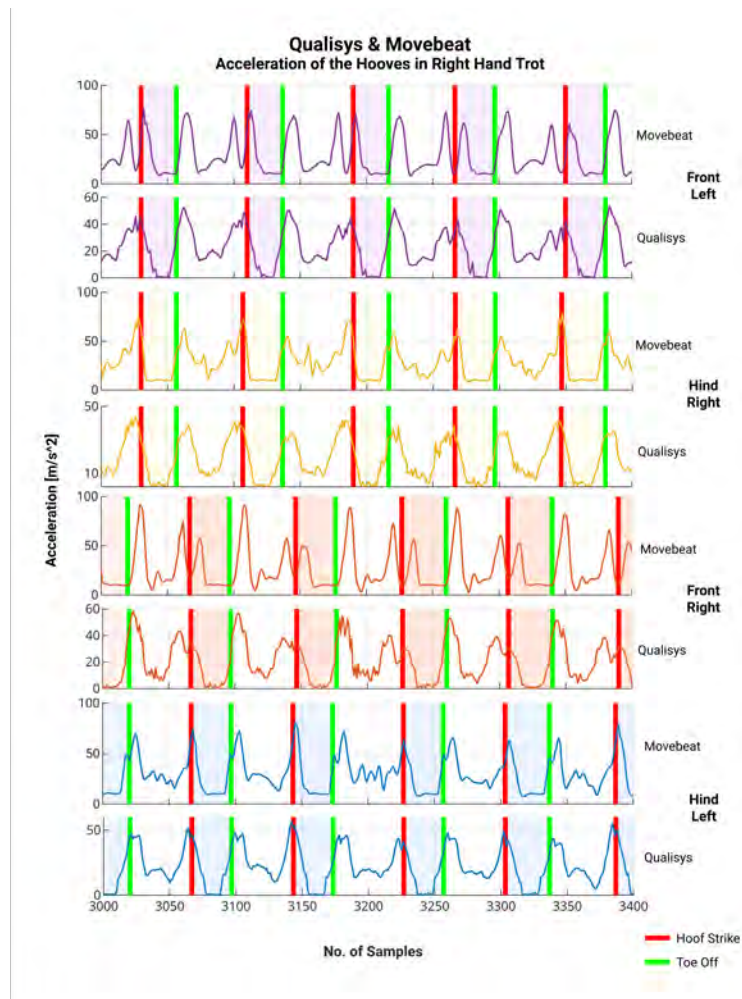


Figure 3.14: The acceleration measurements from the cannons and the hooves using Movebeat’s system with the HS (red) and TO (green) manually verified with Tracker. The gait diagram is displayed in (c)

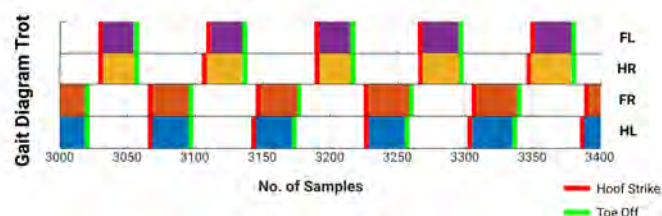
An overview of the acceleration of the hooves using Qualisys and Movebeat is presented in figure 3.15.

One complete stride for front left is visualized from a Qualisys video in figure 3.16. The stride is divided into three parts; Midstance (1) to Terminal Stance (7) in (a), the swing phase from TO (8) to Terminal Swing (21) in (b), and HS (22) to Midstance (26) in (c). Further, the acceleration of the hoof and the cannon for this stride is presented in figure 3.17, both for Qualisys and for Movebeat.

In figure 3.18, one complete stride of hind left is visualized from a video recording by Qualisys. The stride is divided into three parts; Midstance (1) to Terminal Stance (6) in (a), TO (7) to Terminal Swing (20) in (b), and HS (21) to Midstance (22) in (c). The same stride is presented in figure 3.19 as the acceleration of the hooves and cannons, by both Qualisys and Movebeat.

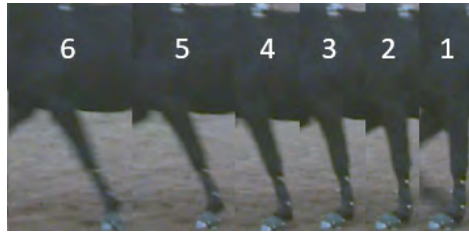


(a) The estimated acceleration from Qualisys and measured acceleration from Movebeat, of the hooves together with HS (red) and TO (green) manually verified with Tracker



(b) The gait diagram of trot

Figure 3.15: The estimated acceleration from Qualisys and measured acceleration from Movebeat, of the hooves together with HS (red) and TO (green) manually verified with Tracker



(a) Midstance to Pre-Swing



(b) Toe Off to Terminal Swing



(c) Initial Contact to Midstance

Figure 3.16: One complete step of front left in trot

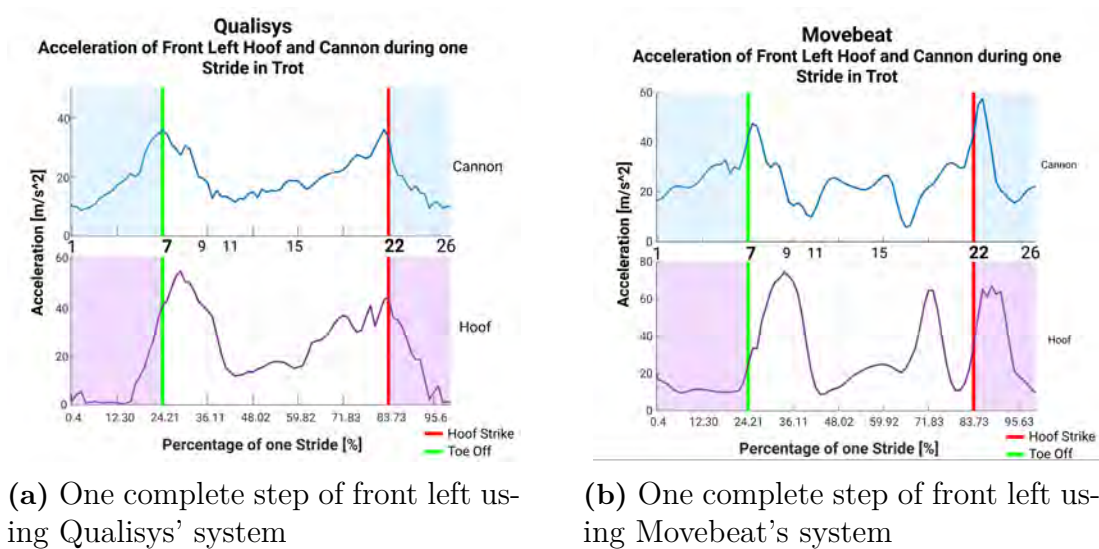


Figure 3.17: The acceleration of front left hoof and cannon using Qualisys' calculated acceleration (a) and Movebeat's measured acceleration (b) in trot

3. Methodology



(a) Midstance to Pre-Swing

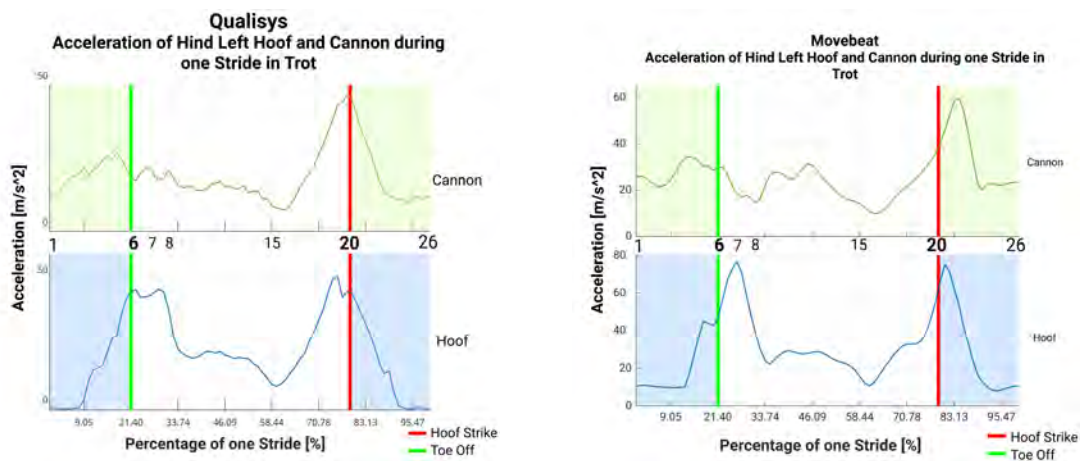


(b) Toe Off to Terminal Swing



(c) Initial Contact to Midstance

Figure 3.18: One complete step of hind left in trot



(a) One complete step of hind left using Qualisys' system

(b) One complete step of hind left using Movebeat's system

Figure 3.19: The acceleration of front left hoof and cannon using Qualisys' calculated acceleration (a) and Movebeat's measured acceleration (b) in trot

4

Results

4.1 Walk

Qualisys' estimated accelerations of the hooves and cannons in walk are displayed in figure 3.6. For the front legs, TO (green) and HS (red) seems to coincide with the two peaks of the gait cycle. For the hind legs, however, it seems that the first peak of the gait cycle occurs slightly after TO, and HS occurs slightly before the second peak of the gait cycle. There is a repeated pattern for the different legs, with difference in the pattern for the front legs and the hind legs. The pattern of the hoof acceleration is similar to the cannon acceleration, when comparing the same legs.

The acceleration measured by Movebeat also follows a pattern, both for the hooves and the cannons figure 3.7. The acceleration peaks seem to coincide with both TO and HS. The acceleration pattern of the hoof seems to differ from the pattern of the cannon, when comparing the same leg, even if there are similarities, e.g. the peaks, and hence TO and HS, seem to coincide.

Figure 3.8 displays the acceleration of the hooves by Qualisys and Movebeat. The patterns of the accelerations of the two systems are similar to each other. However, in the hind leg's acceleration patterns for Movebeat at the moment of TO, there is a minimum between two peaks, while there is no local minimum in the acceleration pattern for Qualisys.

One complete stride of the left front leg is visualized in figure 3.9, and the acceleration of the same stride is presented in figure 3.10, Qualisys

in (a), and Movebeat in (b). The peak of the acceleration of the hoof coincide with TO, for both Qualisys and Movebeat, while HS happens slightly before the peak of accelerations. In Movebeat's acceleration of the hoof, it seems that TO coincides with the local minimum that occurs slightly after the peak. For the cannons, the acceleration peaks slightly before TO and HS. However, Movebeat's acceleration has a local minimum after the peak, that coincides with TO.

Figure 3.11 visualizes one complete stride for hind left, and the acceleration of the same leg and stride is presented in figure 3.12. For the cannons, it seems that HS and TO occur at the peaks of the accelerations, both for Qualisys and Movebeat. However, the pattern for the acceleration for the different systems differs when looking at TO for both hoof and cannon. Movebeat's accelerations have two peaks with one local minimum in between, whereas Qualisys' acceleration has a smoother curvature with one peak. The peak of Qualisys' cannon acceleration seems to coincide with TO, as well as the first peak for Movebeat's hoof acceleration. For the hoof, TO seems to happen slightly before the peak of Qualisys' acceleration, and somewhere in between the first peak of Movebeat's acceleration and the local minimum that occurs slightly after.

Both state of the art, Qualisys, and Movebeat, present a clear walking pattern, both for the acceleration of the hooves and the cannons, figure 3.6 for Qualisys and 3.7. The pattern of the hind legs differs from the pattern of the front legs. By looking at TO and HS, it is easy to see the sequence of walk, HL - FL - HR - FR, and that the walk is a clear four beat rhythm, supported by [9]. Further, there is always at least one hoof on the ground. In figure 3.8, the resemblance between Qualisys and Movebeat's data is clear, however, there are also differences. In Movebeat's data for FL and FR, both TO and HS happens slightly after the acceleration peaks, and for Qualisys' data, TO and HS seem to coincide with the peaks. When looking at the hind legs, the acceleration peaks seem to happen slightly before the acceleration peaks.

4.2 Trot

The acceleration curves for both Qualisys 3.13 and Movebeat 3.14, seem to follow a repeated pattern for each hoof/cannon, and there is a difference in the acceleration pattern of the front legs compared to the hind legs.

In figure 3.15, where both Qualisys' estimated acceleration and Movebeat's measured acceleration are presented, there are repeated patterns for the accelerations given by both of the systems. There is a similarity between both of the system's acceleration patterns, however, there are differences. Movebeat's curves are smoother than Qualisys', and where Qualisys' estimated acceleration shows one peak, e.g. hind left TO, VectorizeMove's measured acceleration has one minor peak, followed by a local minimum, and then a bigger peak, followed by a local minimum and then a peak.

Figure 3.16 presents one complete stride of front left is visualized, and figure 3.17 presents the acceleration of the hoof and cannon for the same leg and stride. The acceleration of the hoof peaks after TO for both Qualisys and Movebeat. The acceleration of the hoof when HS occurs is at a local maximum for Qualisys and slightly before an acceleration peak for Movebeat. An observation is that the estimated acceleration of the hoof by Qualisys peaks slightly after TO, then increases, and then it increases slowly until HS, with the exception of three local minima. Movebeat, on the other hand, presents the acceleration peak slightly after TO, then it decreases rapidly, increases slowly, until there is a peak followed by a minimum, followed by HS and then a peak. The acceleration of the cannon by Qualisys looks smoother than for Movebeat, with two peaks, one at TO and one just before HS. Movebeat's acceleration peaks occur slightly after TO and HS.

However, when looking at Movebeat's data before HS, there is a local maximum followed by a local minimum, and then HS occurs.

One complete stride of hind left is visualized in figure 3.18, and figure 3.17 presents the acceleration of the hoof and cannon for the same leg

and stride. There is a resemblance between the acceleration of the cannon for Qualisys and Movebeat, where the largest peak is around HS. For the hoof, Qualisys presents one peak at TO, and then a minor minimum, and then a peak the same height as the first peak. Movebeat, on the other hand, presents a peak, and then a local minimum, where TO occurs, and then a peak almost double of the size of the first peak. For HS, Qualisys presents one larger peak, followed by a minor local minimum, followed by a minor local maximum, where HS occurs. Movebeat presents one peak, and HS occurs slightly before the peak.

In figures 3.13 - 3.15, the pattern of trot are clear to see. The displayed sequence with the diagonal footfalls (HL + FR) - (HR + FL), and hence with a two beat rhythm, is supported by [9]. Further, the hind legs seem to hit the ground slightly before the front legs in some strides. In this test, the horse was lunged in a circle. If the horse had been trotting in a straight line, the test results might have been different.

In walk, the stance phase was longer than the swing phase for each leg, but in trot the swing phase is longer than the stance phase. Figure 3.8 also reveals a gap between TO for one of the diagonal pairs, to the other diagonal pair's HS, which means that all four legs are in the air (swing phase) at the same time. This is referred to as the suspension phase [9].

5

Discussion and Conclusions

The acceleration patterns for Qualisys' estimated acceleration and Movebeat's measured acceleration, show resemblance, but also differences. One very clear example is for the acceleration of one stride of the front left hoof, figure 3.17, where Movebeat's pattern consists of three major acceleration peaks, whereas Qualisys' pattern shows one peak, then decreases, followed by a slow increasing acceleration, with three local minima, until HS occurs, and then the acceleration seems to decrease again. These differences in the data could be due to the estimation of the acceleration from Qualisys' given positions. Movebeat measures the acceleration, which avoids the risk of losing important data when processing it.

The acceleration patterns of the cannons by Qualisys and Movebeat also seem to differ. Except for data loss, this may also be due to the slightly different placement of the markers and sensors at the cannons. Movebeat's sensors were placed in the middle of the cannons, while Qualisys' sensors were placed anterior (towards the front of the horse), which might have affected the movement of the markers and sensors.

According to table 2.1, and [9], the MCP and the distal interphalangeal of the horse's front limb absorbs energy in the initial ground contact and the loading response, and releases the energy in the terminal stance and pre-swing. By looking at figure 3.16(c), number 22-24, it seems reasonable that there is an absorption in energy in both MCP and the distal interphalangeal. In the terminal stance and the pre-swing, figure 3.16(a) 4-7, display an energy release, in accordance with table 2.1, and [9]. Figure 3.10 indicates that the energy release from the terminal stance and pre-swing converts into an ac-

celeration peak at TO and that the energy absorption in the initial ground contact phase is due to an acceleration peak at HS for the cannon. During the stance phase, however, the acceleration of the cannon seems rather constant, even if there is a change of direction of the cannon, as can be seen in figure 3.16(a) and (c). This can be compared to a ball that falls to the ground, bounces up, and falls back again. The acceleration is constant (9.82 m/s^2), but the direction of the ball changes.

The acceleration peak in figure 3.15(a) after TO for the hoof, is due to the motion of the hoof when lifting from the ground. For the cannon, the peak seems to coincide with TO, but for the hoof the peak is slightly delayed. The acceleration is, however, rising towards its peak before TO. As seen in figure 2.2(b), the angles of the hoof are different in the different phases. Just before TO, the horse lifts the back of the hoof, while the toe stays on the ground. Since the sensor from Movebeat and the marker from Qualisys were placed on the outside/middle of the hoof, viewed from the horse's perspective (can be seen in figure 3.4(a)), the movement of the back of the hoof is measured. Further, after TO the acceleration reaches its peak in the initial swing, probably due to the movement of the hoof, where it first pushes off the ground, and then starts to move forward. The acceleration of the cannon, however, reaches its maximum when the hoof lifts off the ground.

Regarding the hind legs, MCP generates energy in the pre-swing and the initial swing, whilst absorbing energy in the initial contact and loading response, see table 2.2 [9]. Similar to the front leg, the acceleration peaks of the hind leg coincide approximately with TO and HS for the acceleration of the hoof. However, there is only one big peak for the acceleration of the cannon, which coincides with HS. This might indicate that the only time during the trot cycle where there is a great impact of the cannon, is when the hoof strikes the ground (HS).

When comparing the acceleration patterns of the cannons in walk, figure 3.7, and trot, figure 3.14, it seems that the walk would be simpler to find HS and TO, because of the peaks coinciding with these,

especially for the hind legs. However, there are one big peak in the hind cannons, followed by an increase in the acceleration, a plateau and then one local maximum followed by a local minimum. The local minimum seems to coincide with TO. By further study the accelerations in the different directions, x, y, and z, it is possible that there will be a clearer sign of TO.

An optical motion capture system, like Qualisys, gives a high precision when measuring the positions of an object. These positions can be used to estimate the velocity and acceleration. However, there is a risk of losing valuable data due to the estimation. When kinematic signals are of interest, IMU's where the kinematic signals are measured directly, and there is no need for estimation where there is a risk of losing valuable data, is to prefer.

IMU's placed at the cannon can be used to identify the gait phases of walk and trot with accuracy. However, further investigations of the accelerations and the gyros in the different directions, x, y and z, need to be done to easier identify the gait phases.

For the selected tests, there were a consistency of the IMU's identified gait phases. However, the duration of the tests were only 90 s, due to the limitations of the Optical Motion Capture System, since it would bring a too high volume data with longer tests. More studies need to be made to further validate the consistency.

Gaining knowledge of the equine biomechanics, have the potential to increase the welfare of horses and improve their performances. When the quality of the gait can be assessed objectively, with a gait quality index, it can be a valuable tool not only in lameness examinations, but to increase the performance of the horse, and also to improve the riding of our horses.

5.1 Future Work

There is a need of further investigation of the accelerations in the different directions, x, y, and z, to possibly get a more exact moment of TO in trot when placing the IMU on the cannons. The gyro for

the hooves and cannons also need to be further studied, to gain more knowledge in equine biomechanics.

The same analysis for canter needs to be performed, both in right- and left-hand canter. The different phases need to be identified, and not only for the three main gaits in classical riding, but toelt and pace as well. There is a need for studying the different phases in detail, to know exactly what happens, when it happens. The rotations of the hooves and the cannons need to be analysed and compiled into a data base. When this analysis is done, an algorithm can be taught which gait the horse is using.

As [11] stated, there is a need to develop tools in the field of veterinary medicine. When the different movements in the horse's body can be mapped in total, a data base could be compiled with healthy and lame horses. Adding why and where they are lame, AI can be trained to solve our most difficult cases.

Bibliography

- [1] UT Dallas, “Walking in Graphs,” Available at <https://www.utdallas.edu/atec/midori/Handouts/walkingGraphs.htm> (2021/01/18).
- [2] Lexico.com, “Gait | definition of gait by oxford dictionary on lexico.com,” Available at <https://www.lexico.com/definition/gait> (2020/02/03).
- [3] A. Fasano and B. Bloem, “Gait disorders,” *Continuum (Minneapolis, Minn)*, vol. 19, no. 5, pp. 1344–82, 2013. [Online]. Available: <http://www.sciencedirect.com/science/article/pii/S0021929087902661>
- [4] M. Roberts, D. Mongeon, and F. Prince, “Biomechanical parameters for gait analysis: a systematic review of healthy human gait,” *Physical Therapy and Rehabilitation*, vol. 4, no. 6, 2017. [Online]. Available: <https://www.hoajonline.com/physiotherrehabil/2055-2386/4/6>
- [5] J. Mansour and J. Pereira, “Quantitative functional anatomy of the lower limb with application to human gait,” *Journal of Biomechanics*, vol. 20, no. 1, pp. 51 – 58, 1987. [Online]. Available: <http://www.sciencedirect.com/science/article/pii/S0021929087902661>
- [6] S. Khandelwal, “Gait event detection in the real world,” Ph.D. dissertation, Halmstad University, 2018.
- [7] W. Tao, T. Liu, R. Zheng, and H. Feng, “Gait analysis using wearable sensors,” *Sensors*, no. 12, pp. 2255–2283, 2012.

- [8] S. Khandelwal and N. Wickström, “Identification of gait events using expert knowledge and continuous wavelet transform analysis,” in *Proceedings of the International Conference on Bio-inspired Systems and Signal Processing - Volume 1: BIOSIGNALS, (BIOSTEC 2014)*, INSTICC. SciTePress, 2014, pp. 197–204.
- [9] W. Back and H. Clayton, *Equine locomotion*, limited ed. W.B. Saunders, 2001.
- [10] F. S. Bragança], M. Rhodin, and P. [van Weeren], “On the brink of daily clinical application of objective gait analysis: What evidence do we have so far from studies using an induced lameness model?” *The Veterinary Journal*, vol. 234, pp. 11 – 23, 2018. [Online]. Available: <http://www.sciencedirect.com/science/article/pii/S1090023318300066>
- [11] F. Serra Bragança and P. R. van Weeren, “Quantitative gait analysis as an objective tool to determine the functional outcome of musculoskeletal regenerative therapies in horses and dogs,” *Veterinary Sciences*, vol. 37, no. 3, pp. 30–31, Dec 2019. [Online]. Available: <https://www.revistas.una.ac.cr/index.php/veterinaria/article/view/13285>
- [12] S. Bolink, H. Naisas, R. Senden, H. Essers, I. Heyligers, K. Meijer, and B. Grimm, “Validity of an inertial measurement unit to assess pelvic orientation angles during gait, sit–stand transfers and step-up transfers: Comparison with an optoelectronic motion capture system*,” *Medical Engineering & Physics*, vol. 38, no. 3, pp. 225 – 231, 2016. [Online]. Available: <http://www.sciencedirect.com/science/article/pii/S1350453315002672>
- [13] A. I. Cuesta-Vargas, A. Galán-Mercant, and J. M. Williams, “The use of inertial sensors system for human motion analysis,” *Physical Therapy Reviews*, vol. 15, no. 6, pp. 462–473, 2010, pMID: 23565045. [Online]. Available: <https://doi.org/10.1179/1743288X11Y.0000000006>
- [14] A. Snijders MD, B. van de Warrenburg MD, N. Giladi MD, and

- Dr B. Bloem MD, “Neurological gait disorders in elderly people: clinical approach and classification,” *The Lancet*, vol. 6, no. 1, pp. 63–74, 2007.
- [15] T. Lencioni, I. Carpinella, M. Rabuffetti, A. Marzegan, and M. Ferrarin, “Human kinematic, kinetic and emg data during different walking and stair ascending and descending tasks,” *Scientific Data*, vol. 6, no. 309, 2019. [Online]. Available: <https://doi.org/10.1038/s41597-019-0323-z>
- [16] O. J. Woodman, “An introduction to inertial navigation,” University of Cambridge, Tech. Rep., 2007.
- [17] A. Sant’Anna, “A symbolic approach to human motion analysis using inertial sensors : Framework and gait analysis study,” Ph.D. dissertation, Halmstad University, 2012.
- [18] R. M. Alexander, “The gaits of bipedal and quadrupedal animals,” *The International Journal of Robotics Research*, vol. 3, no. 2, 1984.
- [19] M. Hildebrand, “Symmetrical gaits of horses,” *Science*, vol. 191, pp. 701–708, 1965.
- [20] H. Clayton, “Comparison of the stride kinematics of the collected, medium, and extended walks in horses,” *American journal of veterinary research*, vol. 56, pp. 849–52, 07 1995.
- [21] H. M. Clayton, “Classification of collected trot, passage and piaffe based on temporal variables,” *Equine Veterinary Journal*, vol. 29, no. S23, pp. 54–57, 1997. [Online]. Available: <https://beva.onlinelibrary.wiley.com/doi/abs/10.1111/j.2042-3306.1997.tb05054.x>
- [22] M. Holmström, I. Fredricson, and S. DREVEMO, “Biokinematic differences between riding horses judged as good and poor at the trot,” *Equine Veterinary Journal*, vol. 26, no. S17, pp. 51–56, 1994. [Online]. Available: <https://beva.onlinelibrary.wiley.com/doi/abs/10.1111/j.2042-3306.1994.tb04874.x>

- [23] M. Holmström, I. Fredricson, and S. Drevemo, “Variation in angular pattern adaptation from trot in hand to passage and piaffe in the grand prix dressage horse,” *Equine Veterinary Journal*, vol. 27, no. S18, pp. 132–137, 1995. [Online]. Available: <https://beva.onlinelibrary.wiley.com/doi/abs/10.1111/j.2042-3306.1995.tb04905.x>
- [24] ©Cambridge University Press 2020, “Biomechanics | meaning in the cambridge english dictionary,” Available at <https://dictionary.cambridge.org/dictionary/english/biomechanics> (2020/10/22).
- [25] P. L. Cheng and M. Pearcy, “A three-dimensional definition for the flexion/extension and abduction/adduction angles,” *Medical & Biological Engineering & Computing*, vol. 37, no. 4, pp. 440–444, 1999.
- [26] N. J. Dimery, R. M. Alexander, and R. F. Ker, “Elastic extension of leg tendons in the locomotion of horses (equus caballus),” *Journal of Zoology*, vol. 210, no. 3, pp. 415–425, 1986. [Online]. Available: <https://zslpublications.onlinelibrary.wiley.com/doi/abs/10.1111/j.1469-7998.1986.tb03646.x>
- [27] H. W. Merkens and H. C. Schamhardt, “Relationships between ground reaction force patterns and kinematics in the walking and trotting horse,” *Equine Veterinary Journal*, vol. 26, no. S17, pp. 67–70, 1994. [Online]. Available: <https://beva.onlinelibrary.wiley.com/doi/abs/10.1111/j.2042-3306.1994.tb04877.x>
- [28] M. Kutz, *22.3 Optical Motion Capture Systems*. John Wiley & Sons, 2013. [Online]. Available: <https://app.knovel.com/hotlink/khtml/id:kt011AXV4T/handbook-measurement/human-move-introduction>
- [29] A. Baca, “Spatial reconstruction of marker trajectories from high-speed video image sequences,” *Medical Engineering & Physics*, vol. 19, no. 4, pp. 367 – 374, 1997. [Online]. Available: <http://www.sciencedirect.com/science/article/pii/S1350453396000768>
- [30] J. Pezzack, R. Norman, and D. Winter, “An assessment of

derivative determining techniques used for motion analysis,”
Journal of Biomechanics, vol. 10, no. 5, pp. 377 – 382,
1977. [Online]. Available: [http://www.sciencedirect.com/science/
article/pii/0021929077900100](http://www.sciencedirect.com/science/article/pii/0021929077900100)

